we have that $\boldsymbol{E} = 0$ ($\boldsymbol{H} = 0$) in any subregion of Ω implies $\boldsymbol{H} = 0$ ($\boldsymbol{E} = 0$) in the same subregion. Consequently, $\boldsymbol{E} = \boldsymbol{H} = 0$ where $\omega\varepsilon_{\sigma I}(\boldsymbol{r})$ or $\omega\mu_{\sigma I}(\boldsymbol{r})$ are strictly positive. Since in a lossy dielectric $\varepsilon_{\sigma I}(\boldsymbol{r})$ and $\mu_{\sigma I}(\boldsymbol{r})$ cannot be both zero quantities we obtain

$$\boldsymbol{E} = \boldsymbol{H} = 0 \text{ in } \Omega_\sigma. \tag{16}$$

However, (11) does not provide any information about $\boldsymbol{E}$ or $\boldsymbol{H}$ in $\Omega - \Omega_\sigma$, where the dielectric is lossless. Consequently, the following question can be raised: is it possible to have a nonzero field in $\Omega - \Omega$. The answer is no, as proved by Müller [1] (Theorem 34).

In fact, in $\Omega - \Omega_\sigma$ the dielectric is linear and homogeneous, and, as no jump discontinuity in electrical properties is possible, $\boldsymbol{E}, \boldsymbol{H}, \nabla \times \boldsymbol{E}$, and $\nabla \times \boldsymbol{H}$ are continuous. Moreover, $\boldsymbol{E}$ and $\boldsymbol{H}$ satisfy

$$\begin{aligned} \nabla \times \boldsymbol{E} &= -j\omega\mu_u \boldsymbol{H} \\ \nabla \times \boldsymbol{H} &= j\omega\varepsilon_u \boldsymbol{E} \end{aligned} \tag{17}$$

and, by using (16) and the tangential continuity of $\boldsymbol{E}$ and $\boldsymbol{H}$ across dielectric interfaces

$$\left.\begin{aligned} \boldsymbol{n} \times \boldsymbol{E} &= 0 \\ \boldsymbol{n} \times \boldsymbol{H} &= 0 \end{aligned}\right\} \text{ on } S_\sigma. \tag{18}$$

Then ([1], theorem 34) $\boldsymbol{E}$ and $\boldsymbol{H}$ vanish identically in $\Omega - \Omega_\sigma$, i.e.,

$$\boldsymbol{E} = \boldsymbol{H} = 0 \text{ in } \Omega - \Omega_\sigma. \tag{19}$$

Finally, (16) and (19) imply

$$\boldsymbol{E} = \boldsymbol{H} = 0 \text{ in } \Omega \tag{20}$$

and the uniqueness of the solution is proved for the present particular case.

Note that Ω_σ cannot collapse to a point, line or surface; it must be a three–dimensional (3-D) domain bounded by a regular surface.

III. Conclusion

A generalization of the standard uniqueness theorem for time-harmonic electromagnetic fields has been presented and proved. In particular, it has been shown that a linear, lossless, and homogeneous dielectric can be part of the domain of interest. It can be useful to know that, even in this case, the boundary value problem defined by specifying the tangential components of the electric field over the boundary (or the tangential components of the magnetic field over the boundary, or the former components over part of the boundary and the latter components over the rest of the boundary) has a unique solution. However, it will be important to complete this generalization by assuming the linear and lossless dielectric (which is only part of the domain) to be inhomogeneous and even to present jump discontinuities.

References

[1] C. Müller, *Foundations of the Mathematical Theory of Electromagnetic Waves*. Berlin: Springer-Verlag, 1969, pp. 267–331.

[2] R. F. Harrington, *Time-Harmonic Electromagnetic Fields*. New York: McGraw-Hill, 1961, pp. 100–103.

[3] C. A. Balanis, *Advanced Engineering Electromagnetics*. New York: Wiley, 1989, pp. 312–314.

[4] R. E. Collin, *Field Theory of Guided Waves*. New York: McGraw-Hill, 1960, p. 28.

[5] J. A. Stratton, *Electromagnetic Theory*. New York: McGraw-Hill, 1941, pp. 486–488.

Measurement of Simple Resonant Equivalent Circuits for Microstrip Antennas

Steven J. Weiss and Walter K. Kahn

***Abstract*—This paper presents a procedure which can be used to model the input admittance of a probe-fed microstrip antenna using simple circuit components. The values of the components are extracted from experimental data and represent the antenna about any resonant mode. A good circuit description of the antenna can greatly facilitate system analysis.**

I. Introduction

The *cavity model* has been of great value over the years lending practical insight into the operation of microstrip antennas. Using this model, the electromagnetic field between the patch and ground plane of the antenna (the internal field) is assumed to closely resemble the field which would be maintained by a cavity resonator having magnetic walls on the perimeter and the same electric walls as the antenna on the top and bottom [1]–[2]. The resonant modes are dependent on the geometry of the patch. This cavity-like behavior of the internal field(s) suggests that the antennas may be amenable to proven techniques, developed over the years, which are used to characterize the input admittance of cavity resonators.

This paper will develop a procedure by which measured input admittance data may be transformed to a circle of constant conductance. After this transformation is performed, it is a simple matter to realize a resonant circuit which describes the *transformed* data points. Since the transformation itself can be accomplished using circuit elements, a complete circuit description of the antenna's input admittance is obtained.

II. Transformation of the Data

Fig. 1 presents measured admittance data obtained from a probe-fed microstrip antenna using a Hewlett Packard 8720A network analyzer. The circular shape of the data is characteristic of these antennas and not dependent on the geometry of the patch [2]. The center of the circle makes an angle with the horizontal axis of the Smith chart designated by "2θ."

This analysis requires a transformation of the data to a circle of constant conductance. Such a transformation is physically realized using a length of transmission line (for rotation) and an attenuator. That is, the data may be rotated to a position symmetric about the horizontal axis of the Smith chart from the position shown in Fig. 1 if the angle θ is known. This data, symmetric about the horizontal axis, can then be viewed as originating from a circle of constant conductance attenuated by "2α". Accordingly, the transformation of the reflection coefficient data from a circle of constant conductance to a position such as that shown in Fig. 1 is realized from the relation:

$$\Gamma(\omega)_{\text{data}} = e^{-j2\theta} e^{-2\alpha} \Gamma(\omega)_{\text{constant conductance circle}} \tag{1}$$

The values of θ and α are determined from a knowledge of the center and radius of the measured data circle.

Manuscript received January 8, 1996; revised April 19, 1996.

S. J. Weiss is with the U. S. Army Armament Research, Development, and Engineering Center, Adelphi, MD 20783-1197 USA.

W. K. Kahn is with the Department of Electrical Engineering and Computer Science, School of Engineering and Applied Science, The George Washington University, Washington, DC 20052 USA.

Publisher Item Identifier S 0018-9480(96)05643-8.

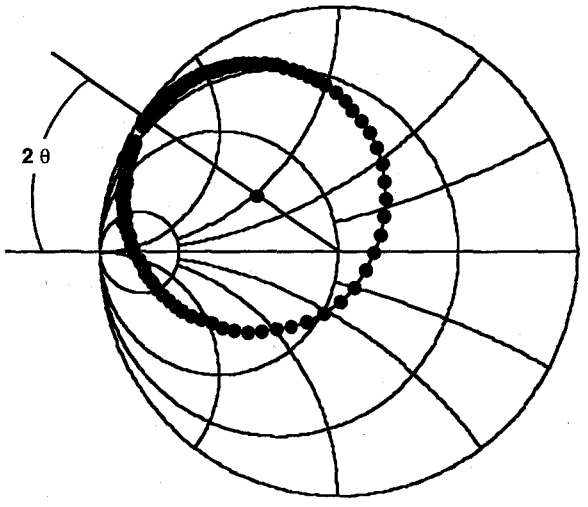

Fig. 1. A typical measured admittance locus of a probe-fed microstrip antenna.

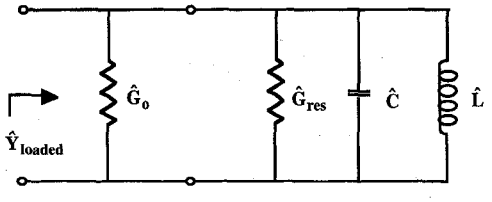

Fig. 2. The loaded input admittance of a tank circuit fed by transmission line.

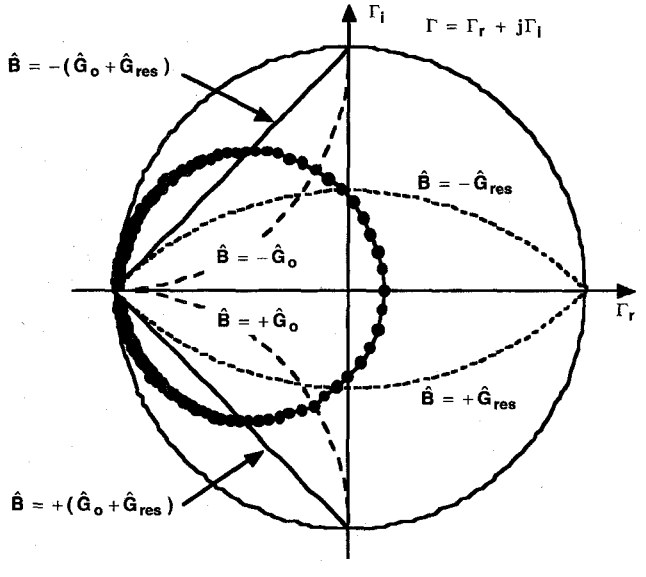

Fig. 3. The location of the Q-specified susceptance values on the Smith chart.

III. Equivalent Circuit of the Transformed Data

The admittance of a resonant circuit consisting of a parallel resistor, capacitor, and inductor lies on a circle of constant conductance. Such a circuit has the negative components of its susceptance mapping to the upper half-plane of the (admittance) Smith chart and positive components mapping to the lower half-plane. As the excitation frequency of the resonant circuit increases, the value of the admittance traverses the constant conductance circle in a clockwise manner. Resonance occurs when the value of the susceptance becomes zero.

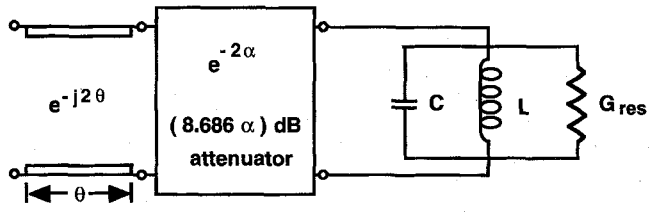

Fig. 4. Equivalent circuit from the measured admittance of a microstrip antenna.

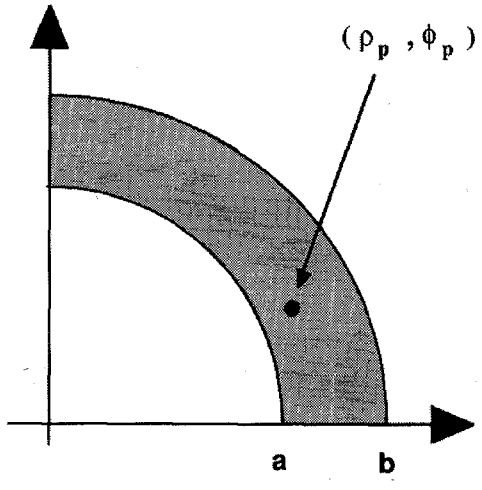

Fig. 5. Geometry of the annular sector antennas.

TABLE I
Anular Position, ϕ_p, for the Annular Sector Antennas

ε_r	d (mils)	ϕ_p (degrees)
2.33	31	38.6
2.33	62	39.1
2.33	125	39.0
4.5	25	38.0
4.5	50	39.0
4.5	100	40.7
6	25	39.0
6	50	38.3
6	100	40.4
10.8	25	36.1
10.8	75	41.4

The measured circularly-shaped admittance data of a microstrip antenna exhibits a similar behavior. It will now be shown that the resonant circuit adequately represents the transformed data points over a range of frequencies *about resonance*. The remaining task is to specify the component values of the resonant circuit. Since the derivation of these values is covered in the literature [3]–[4], only a brief overview of the procedure will be presented.

Consider the circuit shown in Fig. 2. The input admittance of the generator is here considered to be the same as the characteristic conductance of the connecting transmission line, G_o. The input admittance to the circuit (normalized such that $\hat{G}_o = 1$) is written as:

$$\hat{Y}_{\text{loaded}} = \hat{G}_o + \hat{G}_{\text{res}} + j\left(\omega\hat{C} - \frac{1}{\omega\hat{L}}\right). \tag{2}$$

Defining:

$$\hat{Y}_c = \sqrt{\frac{\hat{C}}{\hat{L}}} \quad \text{and} \quad \omega_o = \frac{1}{\sqrt{\hat{L}\hat{C}}} \tag{3}$$

TABLE II
MEASURED VALUES OF Q

d (mils)	ε_r	Q unloaded	Q external	Q loaded
31	2.33	125	129	62
62	2.33	77	58	33
125	2.33	36	61	24
25	4.5	159	190	83
50	4.5	134	126	65
100	4.5	80	137	51
25	6	164	313	104
50	6	165	158	77
100	6	108	108	53
25	10.8	189	176	88
75	10.8	185	372	124

TABLE III
CALCULATED RESONANT CIRCUIT VALUES FOR FIG. 4

d (mils)	ε_r	L (pH)	C (pF)	R_{res} (Ohms)
31	2.33	22.7	150.7	48.3
62	2.33	50.2	69.1	65.4
125	2.33	49.6	73.4	30.4
25	4.5	21.5	296.4	42.7
50	4.5	30.9	202.2	51.6
100	4.5	28.8	221.8	28.4
25	6	15.4	556.7	27.6
50	6	29.9	281.2	53.8
100	6	43.1	197.8	50
25	10.8	34.4	420.6	53.3
75	10.8	16.7	896.5	25.6

TABLE IV
CALCULATED PHASE SHIFT AND ATTENUATION VALUES FOR FIG. 4

d (mils)	ε_r	2θ (Degrees)	α (Napiers)
31	2.33	15.3	0.013
62	2.33	32.8	0.0141
125	2.33	64.4	0.0261
25	4.5	6.29	0.0164
50	4.5	18.5	0.0123
100	4.5	37.1	0.0166
25	6	7.6	0.0157
50	6	16.5	0.0111
100	6	34.6	0.0158
25	10.8	4.5	0.0109
75	10.8	18.2	0.0082

respectively, (2) is written as

$$\hat{Y}_{\text{loaded}} = \hat{G}_o + \hat{G}_{\text{res}} + j\hat{Y}_c\left(\frac{(\omega-\omega_0)(\omega+\omega_0)}{\omega\omega_0}\right). \quad (4)$$

For small changes in frequency (4) simplifies using

$$\Delta\omega = (\omega-\omega_0) \quad \text{and} \quad 2\omega \approx (\omega+\omega_0). \quad (5)$$

Therefore:

$$\hat{Y}_{\text{loaded}} \approx \hat{G}_o + \hat{G}_{\text{res}} + j\hat{Y}_c\left(\frac{2\Delta\omega}{\omega_0}\right). \quad (6)$$

Equation (6) may be written in the following three forms:

$$\hat{Y}_{\text{loaded}} \approx (\hat{G}_o + \hat{G}_{\text{res}})\left[1 + j\frac{\hat{Y}_c}{(\hat{G}_o+\hat{G}_{\text{res}})}\left(\frac{2\Delta\omega}{\omega_0}\right)\right] \quad (7)$$

$$\hat{Y}_{\text{loaded}} \approx \hat{G}_o + \hat{G}_{\text{res}}\left[1 + j\frac{\hat{Y}_c}{\hat{G}_{\text{res}}}\left(\frac{2\Delta\omega}{\omega_0}\right)\right] \quad (8)$$

$$\hat{Y}_{\text{loaded}} \approx \hat{G}_{\text{res}} + \hat{G}_o\left[1 + j\frac{\hat{Y}_c}{\hat{G}_o}\left(\frac{2\Delta\omega}{\omega_0}\right)\right]. \quad (9)$$

Correspondingly, three different values of "Q" may be defined

$$Q_{\text{loaded}} = \frac{\omega_0}{2\Delta\omega} = \frac{\hat{Y}_c}{\hat{G}_o + \hat{G}_{\text{res}}} \quad (10)$$

$$Q_{\text{unloaded}} = \frac{\omega_0}{2\Delta\omega} = \frac{\hat{Y}_c}{\hat{G}_{\text{res}}} \quad (11)$$

$$Q_{\text{external}} = \frac{\omega_0}{2\Delta\omega} = \frac{\hat{Y}_c}{\hat{G}_o}. \quad (12)$$

The respective values of the radian frequency deviation $\Delta\omega$ are defined by the requirement that when (10)–(12) are substituted into (7)–(9), respectively, the real and imaginary components inside the square-bracketed quantities are of equal magnitudes. The values of

the susceptance for the radian frequency deviations become

$$\hat{B}_{\text{loaded}} = \mp(\hat{G}_o + \hat{G}_{\text{res}}) \tag{13}$$

$$\hat{B}_{\text{unloaded}} = \mp\hat{G}_{\text{res}} \tag{14}$$

$$\hat{B}_{\text{external}} = \mp\hat{G}_o. \tag{15}$$

The susceptances specified in (13) to (15), mapped onto the Smith chart, fall on the correspondingly labeled curves shown in Fig. 3. As seen in Fig. 3, the transformed data, coinciding with a circle of constant conductance, intercepts each of these lines once. Since each data point has a frequency associated with it, the values of Q defined in (10) to (12) may be determined from their frequency deviations. The resonant frequency is taken from the data point closest to the value of $\hat{B} = 0$. Since the data is lying on a circle of constant conductance, the value of G_{res} is determined directly. The value of G_o will depend on the input impedances of the instrumentation used to measure the data. Appropriate use of (10)–(12) and (3) will allow determination of $\hat{L}$ and $\hat{C}$:

$$\hat{C} = \frac{(\hat{G}_o + \hat{G}_{\text{res}})Q_{\text{loaded}}}{\omega_0} \quad \hat{L} = \frac{1}{(\hat{G}_o + \hat{G}_{\text{res}})\omega_0 Q_{\text{loaded}}} \tag{16}$$

$$\hat{C} = \frac{\hat{G}_{\text{res}}Q_{\text{unloaded}}}{\omega_0} \quad \hat{L} = \frac{1}{\hat{G}_{\text{res}}\omega_0 Q_{\text{unloaded}}} \tag{17}$$

$$\hat{C} = \frac{\hat{G}_o Q_{\text{external}}}{\omega_0} \quad \hat{L} = \frac{1}{\hat{G}_o\omega_0 Q_{\text{external}}}. \tag{18}$$

The value of $\hat{L}$ and $\hat{C}$ may differ slightly depending on which equation is used. Absolute values are obtained by dividing $\hat{L}$ by G_o and multiplying $\hat{C}$ by G_o. Once the values of G_{res}, L, and C are known, all of the component values of Fig. 2 are fully determined. Fig. 4 illustrates the final equivalent circuit characterizing the input admittance of the microstrip antenna.

IV. Application

This procedure was used to evaluate a variety of microstrip antennas which were fabricated having the shape of an annular sector, Fig. 5. In Fig. 5 the inner radius "a" is given a length of 0.600 inches and the outer radius "b" a length of 1.200 inches. These values held for all of the antennas fabricated for experimental analysis. All of the annular sector antennas had angular spans of 90° with $\rho_p = 0.900$ inches. The dielectric material was procured from Rogers Corporation. Four different materials were used: RT 5870 ($\varepsilon_r = 2.33$), TMM 4 ($\varepsilon_r = 4.5$), TMM 6 ($\varepsilon_r = 6.0$), and RT 6010 ($\varepsilon_r = 10.8$).

The dielectric constants for the materials, substrate thicknesses "d," and probe positions for the various antennas are given in Table I.

Using the analysis outlined in this paper, measured values of Q were obtained for each antenna, Table II. The measured values of Q are in good agreement with values obtained by us using other measurement techniques. The values of the components for the resonant circuit were then found using data Table II and (16) to (18). The absolute values of the circuit parameters of Fig. 4 are given in Table III. The values of the phase shift and the attenuation are given in Table IV.

V. Conclusion

This paper adapts some experimental techniques originally developed to model the admittance of cavity resonators and applies them to microstrip antennas. The application requires a transformation of the data to a constant conductance circle which is physically realized using a length of transmission line and an attenuator. The admittance calculated from the equivalent circuit was found to closely match the measured data verifying the model within the range of frequencies for which the various values of Q were measured. The equivalent circuit demonstrates that simple and accurate models of these antennas may be easily constructed. The equivalent circuits can prove quite valuable when computer simulations are required.

Acknowledgment

The authors wish to thank the U.S. Army Armament Research, Development and Engineering Center in Adelphi, MD for the use of their facilities.

References

[1] W. F. Richards, Y. T. Lo, and D. D. Harrison, "Theory and experiment on microstrip antennas," *IEEE Trans. Antennas Propagat.*, vol. AP-27, pp. 137–145, Mar. 1979.

[2] Y. T. Lo, D. Solomon, and W. F. Richards, "An improved theory for microstrip antennas with applications," *IEEE Trans. Antennas Propagat.*, vol. AP-29, no. 1, pp. 38–46, Jan. 1981.

[3] J. L. Altman, *Microwave Circuits*. Princeton, NJ: Van Nostrand, 1964.

[4] G. H. Owyang, *Foundations for Microwave Circuits*. New York: Springer-Verlag, 1989.